

Creep Crack Growth Properties of Low Pressure Turbine Rotor Steel under Constant Load and C_t

Soon-Uk Jeong

School of transport vehicle engineering, Gyeongsang National University, Kyongnam, South Korea

ABSTRACT

The propagation rate(da/dt) prediction parameter and the microstructure properties of creep crack in domestic 3.3NiCrMoV steel were investigated at 550°C by using 0.5" CT specimen under constant load(4090N) and constant C_t (300~4000N/mhr) condition that was maintained during crack growth of 1mm distance. C^* usually increased with crack length though load was reduced in order to maintain constant C_t value as crack growth and considerably showed the scatter band, but C_t depended on load line displacement rate and represented a good relation with da/dt . At constant load and C_t region, crack growth slope was 0.900 and 0.844 each, on the other hand C^* slope was 0.480.

Fully coalesced area(FCA) ahead of crack tip was increased as C_t value increase to the critical value, and after that value FCA decreased. The average diameter distribution of cavity in FCA showed the greatest value about 1.5 μm when $C_t=2000\text{N/mhr}$. The increasing of C_t in FCA view point enlarged the size of damage area and the size reached to maximum 800 μm when $C_t=2000\text{N/mhr}$.

Keywords : Fully Coalesced Area, Creep Crack Growth Rate, Load Line Displacement Rate, Creep-induced Displacement

1. Introduction

Each component of the equipment used in the high temperature and the high pressure atmosphere accompanies creep deformation. The life of material may be consisted of the crack initiation and the crack propagation⁽¹⁻³⁾, and the commerce products have a possibility that the crack is indwelled during the manufacture process or the use, and initiation, growth and combination of the cavity are happened by the relative stress concentration in this crack front, and the sudden fracture is caused by the rapid propagation of crack⁽⁴⁾. So far the stress intensity factor(K), J-integral, C^* -integral and C_t have been used as the parameter⁽⁵⁻⁷⁾ to predict the creep crack growth rate(da/dt). According to the report⁽⁷⁾, K is a suitable parameter in case of the ferrite group steels that is strong for creep brittleness and Ni-based heat resistant alloy that is strong at high temperature. J-integral is suitable as the load

parameter⁽⁸⁾ for SUS316 steel which comparatively cause a large plastic region in the crack front. And, C^* -integral⁽⁹⁾ is well applied for the material that HRR stress field was formed because of the wide deformation by power law creep. But, K, J-integral, C^* -integral and so on appear a situation of the direct opposition according to specimen profile or creep region. Lately C_t was proposed to predict da/dt in several environment including small scale and transient creep⁽¹⁰⁾.

This thesis studied the properties of C^* -integral and C_t parameter under constant load and constant C_t condition through da/dt experiment, and investigated the change of crack front damage region and creep crack growth properties through the fracture surface analysis by using 3.3NiCrMoV steel used to the low pressure rotor of fossil power plant.

2. Experimental method

The material that is used to the experiment is developed

Table 1 Chemical composition of 3.3NiCrMoV steel.

C	Si	Mn	Ni	Cr	Mo	V	P	S
0.28	0.25	0.35	3.32	1.34	0.29	0.09	0.005	0.003

Table 2 Mechanical properties of 3.3NiCrMoV steel at room temperature

Tensile strength (MPa)	Yield strength (MPa)	Elongation (%)	Reduction of area (%)	Hardness (H _{RC})
856	745	10.8	21.8	25

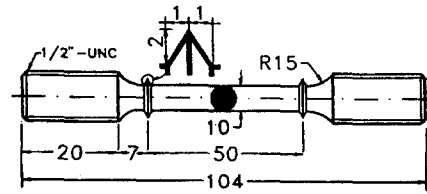
at domestic H heavy industry Co. and melted in the induction furnace(Toccol-227) as 3.3%NiCrMoV steel that was the low pressure rotor material used to the fossil plant. And, after annealing and oil quenching for 1 hour in 1100 °C, as tempering for 5 hours in 690 °C, the final structure appeared tempered-martensite structure (grain size ASTM No. 4).

Chemical composition and mechanical properties of the material were summarized in Table 1 and Table 2. The specimens were machined as Fig. 1 with 0.5" CT (compact tension) type. And, 20 pre-test specimens were prepared for the crack length verification by DC electric potential method^{4,11)}.

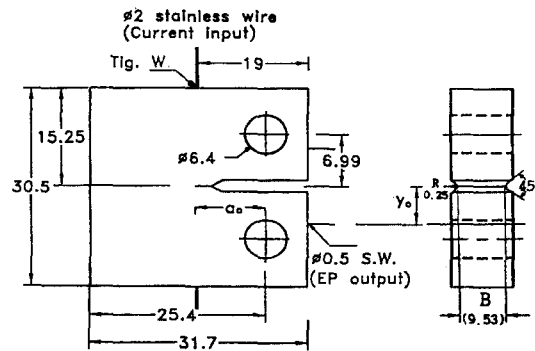
After the test was discontinued during the examination, the specimens were brittle-fractured in the liquid nitrogen and divided as 8 partitions for the thickness direction according to ASTM E399 specification, and the crack growth rate and the final crack length by third dimension universal profile test of 0.1 μm accuracy were measured.

The voltage input and output terminal was welded for TIG by the stainless wire to keep away the oxidation by the high temperature as long as possible. And, the heat electromotive forces showed some differences according to the test piece but appeared about -10 ~ -50 μV, and turn off the current in fixed period(10 minutes) during the examination and calculated the crack length by considering electromotive forces.

The test piece was pre-cracked to 8mm by 7Hz sine wave under the maximum load(11kN) and the minimum load(1.1kN) as universal fatigue test machine(Instron model 1350) according to ASTM E813 specification, and processed the side groove by 25% depth of the thickness to both of test piece so that the plain strain condition



(a) uniaxial creep



(b) crack growth creep

Fig. 1 Uniaxial and constant C₁ creep specimen profile

could be kept well.

Constant C₁ test condition was shown in Table 3. Because constant C₁ test must reduce the applied load according to the crack growth, the digital stress relaxation apparatus that is attached to single lever type creep tester was used.

The applied load was automatically inputted after the crack length by DC potential method was calculated at 1 second interval during test.

The temperature was kept within ±2 °C by using 3-zone asbestos resistance furnace, and the load point

Table 3 Test condition of constant load and constant C₁

Applied constant load (N)	Initial condition		Constant C ₁		
	Crack length (mm)	Stress intensity factor (MPa√m)	Value (N/mhr)	Start time (hr)	Hold time (hr)
4,090	12.70	24.86	300	18.1	17.5
			1,000	35.4	6.3
			2,000	54.3	4.5
			4,000	61.5	2.5

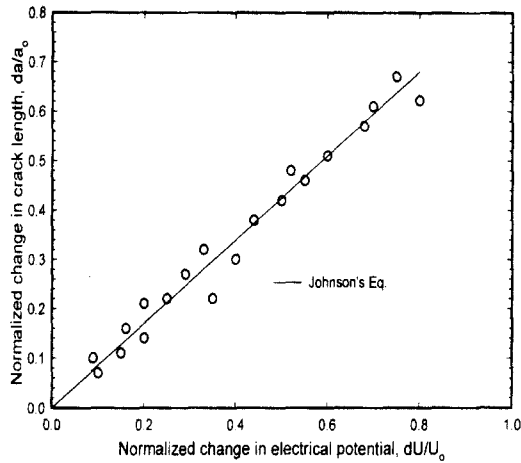


Fig. 2 Relationship between the change in crack length and the change in electrical potential for 0.5T-CT specimen at 550 °C

displacement was measured by high temperature extensometer.

Constant C , value in this experiment was held as 300, 1000, 2000 and 4000N/mhr. After the load was kept until the crack grew about 1mm, removed the load and cut the side groove by grinding and observed the cavity by optical microscope. The remained ligament was split by brittle fracture in the liquid nitrogen, and investigated the distribution situation and the size of cavity by SEM and image analyzer at the crack front and the fracture surface.

3. Experimental results

3.1 Verification of the creep crack length

The measurement results of creep crack length by using DC potential methods between the voltage change ($dU=U-U_0$) about initial voltage (U_0) and the crack length change ($da=a-a_0$) about initial crack length (a_0) could be plotted as Fig. 2. The theoretical analysis by Johnson¹¹⁾ agreed well with the experiment results as following.

$$\frac{U}{U_0} = \frac{\cosh^{-1} \left\{ \frac{\cosh(\pi y_0/2W)}{\cos(\pi a/2W)} \right\}}{\cosh^{-1} \left\{ \frac{\cosh(\pi y_0/2W)}{\cos(\pi a_0/2W)} \right\}} \quad (1)$$

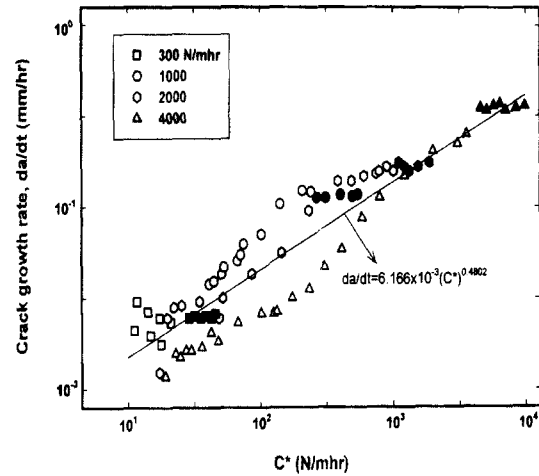


Fig. 3 Relationship between C^* and crack growth rate

Where W is the test piece width(mm), a_0 is the initial crack length(mm) and y_0 is a half of the voltage output distance(mm).

3.2 C^* parameter

C^* -integral can be calculated by multi-specimen¹²⁾, J-integral analysis method¹³⁾ and area method¹⁴⁾ etc. According to Saxena⁷⁾, he reported that C^* -integral included the plastic deformation considering pure bending and tension at the same time, and the following equation was valid after the applied load(P) and the load line displacement rate($\dot{\Delta}$) were measured in precracked CT specimen.

$$C^* = \frac{n}{n+1} \frac{P\dot{\Delta}}{B(W-a)} \left[\gamma - \frac{\beta}{n} \right] \quad (2)$$

Where n is the creep exponent acquired by the experiment, $n = 7.225$ for 3.3%NiCrMoV steel. α , β and γ are the material constant as following.

$$\gamma = \frac{2(1+a)(1+a/W)/(1+a^2) + \alpha(1-a/W)}{(1+a/W) + \alpha(1-a/W)}$$

$$\beta = \frac{\alpha}{\alpha + (1+a/W) + \alpha(1-a/W)}$$

$$\alpha = \sqrt{[2a/(W-a)]^2 + 2[2a/(W-a)] + 2 - [2a/(W-a) + 1]}$$

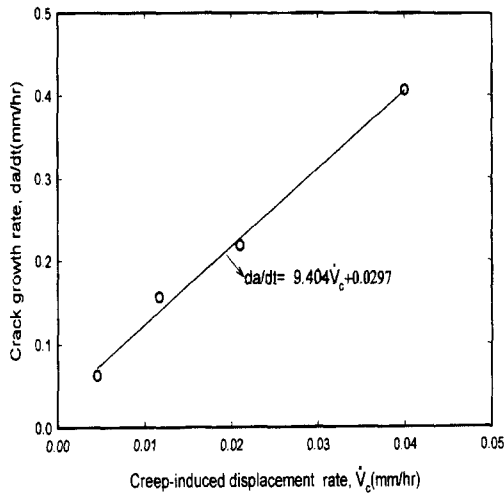


Fig. 4 Relationship between creep-induced displacement rate and crack growth rate

In the case of this experiment, the change of C^* -parameter was shown in Fig. 3. Because C^* -parameter is the load line displacement function, C^* value show gradually increasing aspects under the constant C_t condition. That reason is considered that Δ is increased rapidly in the tertiary creep stage.

Excepting constant C_t part, the experiment result was as following if it was represented as the correlation of da/dt and C^* by the linear regression analysis.

$$da/dt = 6.166 \times 10^{-3} (C^*)^{0.4802} \quad (3)$$

The application result of C^* can see that the data band is fairly scatter according to applied load as Fig. 3. Therefore, C^* is considered that it is not a suitable parameter to predict da/dt . This tendency was shown by da/dt test of 800H alloy steel at 650 °C in case the changed stress ratio and frequency according to Hour's research¹⁵⁾. And though C^* application decreased the scatter band of data than σ_{net} and K_{max} , but the data was not together crowded on one straight line, Effect of the application load was clearly shown in case of the transient region.

3.3 C_t parameter

C^* -integral is a parameter to consider W and not to

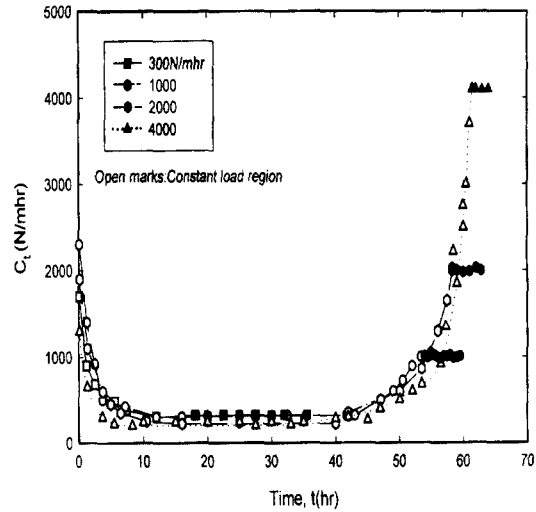


Fig. 5 The variation of C_t with time under constant load and constant C_t

consider the creep-induced displacement rate (\dot{V}_c). Therefore, C^* is not appropriate to predict da/dt quantitatively except the steady state creep according to material. C_t that is proposed for the creep crack growth analysis by Saxena⁷⁾ is as following.

$$C_t = \frac{P \dot{V}_c}{BW} \frac{F'}{F} + C^* \left[1 - \frac{F'}{F} \right] \quad (4)$$

Where $V_c = V^o - V_o = Pr_c dC/da$

$$\dot{V}_c = \frac{4\zeta(1-\nu^2)}{E(n-1)} \left(\frac{P}{B} \right)^3 \frac{F^4}{W^2} t^{3-n/n-1} (EA)^{2/(n-1)}$$

$$\zeta = \frac{1}{2\pi} \left[\frac{(n+1)^2}{2n \cdot \beta^{n+1}} \right]^{2/(n-1)}$$

Where P is the action load, V_o is displacement, V^o is all displacement, r_c is creep size and C is the elasticity compliance. And, $F = F(a/W) = (K/P)BW^{1/2}$ being K -calibration factor⁷⁾, $F' = dF/d(a/W)$ means the calibration factor that depends on n . ν is Poisson ratio, A is the creep exponent and E is the elastic modulus. And, β^{n+1} is reported that the value appear to 0.69 about $3 \leq n \leq 10$ ¹⁶⁾.

In the meantime, the relationship between da/dt and \dot{V}_c was shown in Fig. 4 and the slope appeared about 9.404. Because the constant \dot{V}_c is shown in case of constant C_t , constant C_t test can indirectly know that constant da/dt is presented.

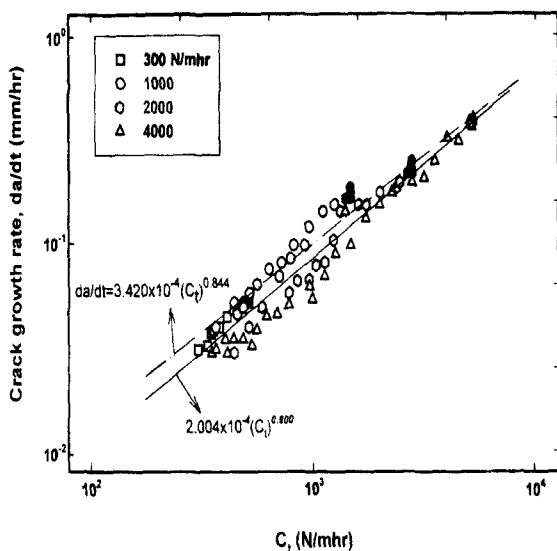


Fig. 6 Relationship between C_1 and crack growth rate

C_1 change according to the creep time was shown in Fig. 5 under constant load and constant C_t condition.

The reason that creep crack growth rate (da/dt) gradually becomes to be low in the transient region of test is due to the work hardening phenomenon by creep deformation. The elastic deformation around crack according to the time passage is gradually reduced by the creep deformation and stay in the stable state along with the time passage. Therefore, da/dt and \dot{V}_c are considered as looking the fixed tendency at this time.

17.5, 6.3, 4.5, 2.5hrs holding under $C_1 = 300, 1000, 2000, 4000$ N/mhrs induced the crack to grow about 1mm. Crack about 20%(1mm) of whole crack length(5~6mm) is considered that it is enough length to remove the test effect performed under constant load. According to Hong's research, he reported that the damage zone size was about 200 μm under the constant load test of $C_1 = 50 \sim 5500$ (N/mhr).

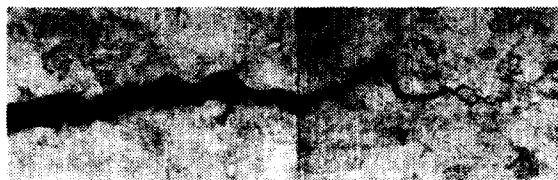
Under 4-kinds constant C_1 condition, the result of da/dt experiment was shown in Fig. 6. The relationship between C_1 and da/dt was presented a linear function as following.

$$da/dt = 3.420 \times 10^{-4} (C_1)^{0.844} \quad (5)$$

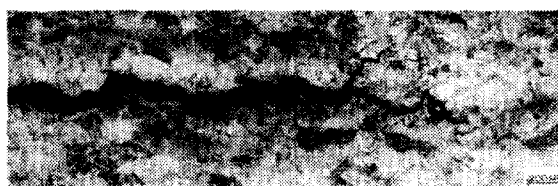
In the meantime, the equation was expressed as



(a)



(b)



(c)

Fig. 7 The Shape of propagated crack under constant C_1 condition (a) 300N/mhr, (b) 2000 N/mhr, (c) 4000N/mhr

following if the experiment data was arranged by the linear regression analysis except constant C_1 condition.

$$da/dt = 2.004 \times 10^{-4} (C_1)^{0.900} \quad (6)$$

Under constant load and constant C_1 , the experiment result was similarly presented, therefore the constant C_1 experiment could be existed in extension of the constant load test, and the application of C_1 is also valid in the constant load test. This result agreed well with Saxena's study⁷⁾ reporting for 1%CrMoV steel that da/dt crowds together in a straight line regardless of the applied load, the temperature and the load rate in case of the experiment of 482°C and 538°C air.

3.4 Fracture surface examination

After C_1 creep test was completed (crack length 6~8mm), the test piece removed side groove, and the fracture surface observed by microscope was shown in Fig. 7. All cracks were propagated along with the grain boundary.

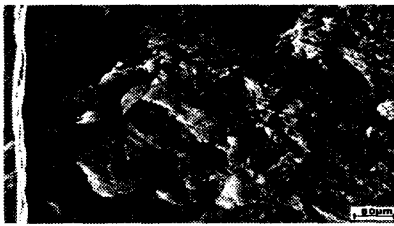


Fig. 8 Intergranular fractured surface at vicinity of crack tip under $C_t=300\text{N/mhr}$

In case low C_t value about 300N/mhr of (a), crack comparatively showed the low growth rate aspect that end region of the crack involved the discontinuity, and in case $C_t = 4000\text{ N/mhr}$ of (b), the microcrack showed the continuous sharp properties that is linked to one by the major crack. And, the fracture surface of (c) showed a complex mode.

In case $C_t=2000\text{ N/mhr}$, the size of crack damage zone was investigated to study the crack size and distribution within border of the region between creep and impact zone of specimen which is brittle-fractured in the liquid nitrogen.

The creep fracture surface showed fully coalesced area (FCA) as photograph shown in Fig. 8, The average diameter distribution of cavity in FCA was shown in Fig. 9 and the average diameter of cavity was the greatest value about $1.5\ \mu\text{m}$ when $C_t=2000\text{N/mhr}$. The damage size of crack front was shown in Fig. 9 at the same time. The increasing of C_t in FCA view point enlarged the size of damage area, and the size reached the maximum value about $800\ \mu\text{m}$ when $C_t=2000\text{N/mhr}$.

The close relationship was existed in between the average diameter and the creep damage area zone. Therefore, The increase of C_t means the enlargement of creep deformation area size, the size of damage area is considered that it is preferably decreased because the crack growth rate is higher than the formation of deformation field if C_t value exceeds any critical value.

In view of the results so far achieved, stress concentration more than suitable creep size that equal to C_t value in the small area of crack tip field is instantaneously formed at crack front in case the reach of stress level equivalent to C_t value, and the stress of this region is reduced by the deformation according to the creep time passage.

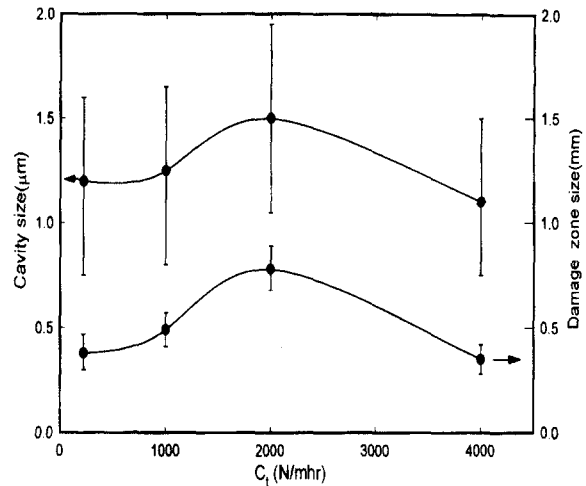


Fig. 9 The variation of cavity size and damage zone size with C_t

If the stress level stay in the corresponded C_t value, the deformation field of crack front was increased. Cavities are created, grown and combined in these deformation field, and these deformation keep the fixed size according to crack growth if the constant C_t is kept, and da/dt is considered that it hold the fixed value because of staying in constant deformation.

4. Conclusions

The results measured crack growth rate (da/dt) of low pressure steam turbine rotor material, 3.3NiCrMoV steel under the constant load and the constant C_t creep test were as following.

- 1) C_t parameter had a close interrelationship with induced-deformation rate and C^* was gradually increased under constant C_t state.
- 2) da/dt estimation by C^* is not suitable because the effect of applied load was clearly showed.
- 3) da/dt by C_t was crowded in a uniform straight line regardless of the applied load, da/dt under constant C_t condition showed the aspect that was together crowded.
- 4) According to the constant C_t test result in case $C_t=2000\text{N/mhr}$, the cavity size and the damage area showed the greatest value, and these data presented the close relationship mutually.

Acknowledgement

This work was supported by the Brain Korea 21 Project.

References

1. Sellars, C. M., "Creep Strength in Steel and High Temperature Alloys," pp. 20, 1974.
2. Baek, N. J., Lee, S. B., and Lee, M. W., "A Study on the Creep Mechanism of 316 Stainless Steel under High Stresses," Journal of Korean Society of Precision Engineering, Vol. 2, No. 1, pp. 53-61, 1987.
3. Lee, K. Y., and Kim, J. S., "Stress Analysis of Creep Material Including Elliptical Rigid Inclusion by Complex Pseudo-Stress Function," Proceeding of the JKSP E 1997 Fall Annual Meeting pp. 740-743, 1997.
4. Sur, S. W., Sin, Y. S., and You, H. I., "A Study on the Fatigue Crack growth," Journal of Korean Society of Precision Engineering, Vol. 9, No. 1, pp. 106-117, 1992 .
5. Baek, U. B., Yoon, K. B., Lee, H. M., and Suh, C. M., "Creep-Fatigue Crack Growth at CrMo Steel Weld Interface," Journal of the Korean Society of Mechanical Engineers(A), Vol. 24, No. 12, pp. 3088-3095, 2000.
6. Yoon, K. B., Kim, K. W., and Baek, U. B., "Modeling of Creep Crack Growth Behavior of Low-Alloy Steel Weld," Journal of the Korean Society of Mechanical Engineers(A), Vol. 22, No. 12, pp. 2153-2162, 1998.
7. Saxena, A., "Creep Crack Growth under NonSteady State Conditions," Fracture Mechanics, ASTM STP905, pp. 185-201, 1986.
8. Taira, S., Ohtani, R., and Komatsu, T., "Application of J-Integral to High Temperature Crack Propagation(Part I - Fatigue Crack propagation)," Journal of Engineering Materials and Technology, Vol. 101, pp. 154-161, 1979.
9. Hutchinson, J. W., "The Mechanics and Physics of Solids," Vol. 16, pp. 337-347, 1968.
10. Saxena, A., Han, J., and Banerji, K., "Creep Crack Growth Behavior in Power Plant Boiler and Steam Pipe Steels," Journal of Pressure Vessel Technology, Vol. 110, pp. 137-146, 1988.
11. Schwalbe, K. H., and Hellmann, D., "Application of the Electrical Potential Method to Crack Length Measurements Using Johnson's Formula," JTEVA, Vol. 9, No. 3, pp. 218-221, 1981.
12. Saxena, A., "Evaluation of C* for the Characterization of Creep-Crack-Growth Behavior in 304 Stainless Steel," Fracture Mechanics, Twelfth Conference, ASTM STP700, pp. 131-151, 1980.
13. Ernst, H. A., "Unified Solution for J Ranging Continuously from Pure Bending to Pure Tension," Fracture Mechanics, Vol. 1, ASTM STP791, pp. 1499-1519, 1983.
14. Hermann, R., "Fracture at High Temperature," SpringerVerlag, pp. 263-298, 1986.
15. Hour, K. Y., and Stubbins, J. F., "Fatigue Crack Growth Behavior of Alloy 800H at Elevated Temperature," Journal of Engineering Materials and Technology, Vol. 113, pp. 271-279, 1991.
16. Tada, H., Paris, P., and Irwin, G. R., "The Stress Analysis of Cracks Handbook," Del Research Corp., Hellertown, 1973.
17. Hong, S. H., "Creep Crack Growth and Micromechanism," KAIST, Ph.D, 1989.